

# The Unbalanced Gromov Wasserstein Distance: Conic Formulation and Relaxation

Thibault Séjourné  
ENS, PSL University  
thibault.sejourné@ens.fr

François-Xavier Vialard      Gabriel Peyré  
LIGM, Univ Gustave Eiffel, CNRS      CNRS, ENS, PSL University  
francois-xavier.vialard@u-pem.fr      gabriel.peyre@ens.fr

March 3, 2022

## Abstract

Comparing metric measure spaces (i.e. a metric space endowed with a probability distribution) is at the heart of many machine learning problems. This includes for instance predicting properties of molecules in quantum chemistry or generating graphs with varying connectivity. The most popular distance between such metric measure spaces is the Gromov-Wasserstein (GW) distance, which is the solution of a quadratic assignment problem. This distance has been successfully applied to supervised learning and generative modeling, for applications as diverse as quantum chemistry or natural language processing. The GW distance is however limited to the comparison of metric measure spaces endowed with a *probability* distribution. This strong limitation is problematic for many applications in ML where there is no a priori natural normalization on the total mass of the data. Furthermore, imposing an exact conservation of mass across spaces is not robust to outliers and often leads to irregular matching. To alleviate these issues, we introduce two Unbalanced Gromov-Wasserstein formulations: a distance and a more tractable upper-bounding relaxation. They both allow the comparison of metric spaces equipped with arbitrary positive measures up to isometries. The first formulation is a positive and definite divergence based on a relaxation of the mass conservation constraint using a novel type of quadratically-homogeneous divergence. This divergence works hand in hand with the entropic regularization approach which is popular to solve large scale optimal transport problems. We show that the underlying non-convex optimization problem can be efficiently tackled using a highly parallelizable and GPU-friendly iterative scheme. The second formulation is a distance between mm-spaces up to isometries based on a conic lifting. Lastly, we provide numerical simulations to highlight the salient features of the unbalanced divergence and its potential applications in ML.

# 1 Introduction

Comparing data distributions on different metric spaces is a basic problem in machine learning. This class of problems is for instance at the heart of surfaces [4] or graph matching [42] (equipping the surface or graph with its associated geodesic distance), regression problems in quantum chemistry [21] (viewing the molecules as distributions of points in  $\mathbb{R}^3$ ) and natural language processing [24, 1] (where texts in different languages are embedded as points distributions in different vector spaces). This paper defines for the first time a class of distances between these objects, which we define below as metric measure spaces.

**Metric measure spaces.** The mathematical way to formalize these problems is to model the data as *metric measure spaces* (mm-spaces). A mm-space is denoted as  $\mathcal{X} = (X, d, \mu)$  where  $X$  is a complete separable set endowed with a distance  $d$  and a positive Borel measure  $\mu \in \mathcal{M}_+(X)$ . For instance, if  $X = (x_i)_i$  is a finite set of points, then  $\mu = \sum_i m_i \delta_{x_i}$  (here  $\delta_{x_i}$  is the Dirac mass at  $x_i$ ) is simply a set of positive weights  $m_i = \mu(\{x_i\}) \geq 0$  associated to each point  $x_i$ , which accounts for its mass or importance. For instance, setting some  $m_i$  to 0 is equivalent to removing the point  $x_i$ . We refer to [37] for a mathematical account on the theory of mm-spaces.

In all the applications highlighted above, it makes sense to perform the comparisons up to isometric transformations of the data. Two mm-spaces  $\mathcal{X} = (X, d_X, \mu)$  and  $\mathcal{Y} = (Y, d_Y, \nu)$  are considered to be equal (denoted  $\mathcal{X} \sim \mathcal{Y}$ ) if they are isometric, meaning that there is a bijection  $\psi : \text{spt}(\mu) \rightarrow \text{spt}(\nu)$  (where  $\text{spt}(\mu)$  is the support of  $\mu$ ) such that  $d_X(x, y) = d_Y(\psi(x), \psi(y))$  and  $\psi_\# \mu = \nu$ . Here  $\psi_\#$  is the push-forward operator, so that  $\psi_\# \mu = \nu$  is equivalent to imposing  $\nu(A) = \mu(\psi^{-1}(A))$  for any set  $A \subset Y$ . For discrete spaces where  $\mu = \sum_i m_i \delta_{x_i}$ , then one should have  $\nu = \psi_\# \mu = \sum_i m_i \delta_{\psi(x_i)}$ . As highlighted by [28], considering mm-spaces up to isometry is a powerful way to formalize and analyze a wide variety of problems such as matching, regression and classification of distributions of points belonging to different spaces. The key to unlock all these problems is the computation of a distance between mm-spaces up to isometry. So far, existing distances (reviewed below) assume that  $\mu$  is a probability distribution, i.e.  $\mu(X) = 1$ . This constraint is not natural and sometimes problematic for most of the practical applications to machine learning. The goal of this paper is to alleviate this restriction.

**Csiszár divergences** The simplest case is when  $X = Y$  and one simply ignores the underlying metric. One can then use Csiszár divergences (or  $\varphi$ -divergences), which perform a pointwise comparison (which should be contrasted to optimal transport distances, which perform a displacement comparison). It is defined using an entropy function  $\varphi : \mathbb{R}_+ \rightarrow [0, +\infty]$ , which is a convex, lower semi-continuous positive function satisfying  $\varphi(1) = 0$ . Its associated recession constant is  $\varphi'_\infty \stackrel{\text{def.}}{=} \lim_{r \rightarrow \infty} \varphi(r)/r \in \mathbb{R} \cup \{+\infty\}$ . For any  $(\mu, \nu) \in \mathcal{M}_+(X)^2$ , we write the

Lebesgue decomposition as  $\mu = \frac{d\mu}{d\nu}\nu + \mu^\perp$ . The Csiszár  $\varphi$ -divergence is defined as

$$D_\varphi(\mu|\nu) \stackrel{\text{def.}}{=} \int_X \varphi\left(\frac{d\mu}{d\nu}\right) d\nu + \varphi'_\infty \int_X d\mu^\perp. \quad (1)$$

This divergence  $D_\varphi$  is convex, positive, 1-homogeneous and weak\* lower-semicontinuous, see [26] for details. One can reverse it in the sense  $D_\varphi(\mu|\nu) = D_\psi(\nu|\mu)$  where  $\psi$  is the reverse entropy defined as  $\psi(r) = r\varphi(1/r)$ ,  $\psi(0) = \varphi'_\infty$  and  $\psi'_\infty = \varphi(0)$ . Particular instances of  $\varphi$ -divergences are Kullback-Leibler (KL) for  $\varphi(r) = r \log(r) - r + 1$  (note that here  $\varphi'_\infty = \infty$ ), the Total Variation (TV) for  $\varphi(r) = |r - 1|$  and the Hellinger distance for  $\varphi(r) = (\sqrt{r} - 1)^2$ . The indicator divergence  $D_\varphi(\mu, \nu) = +\infty$  for  $\mu \neq \nu$  and 0 otherwise is obtained by using  $\varphi(r) = \iota_=(r)$  which is 0 if  $r = 1$  and  $+\infty$  otherwise.

**Balanced and unbalanced optimal transport.** If the common embedding space  $X$  is equipped with a distance  $d(x, y)$ , one can use more elaborated methods, and in particular consider optimal transport (OT) distances, which can be computed by solving convex optimization problems. This type of methods has proven useful for ML problems as diverse as domain adaptation [15], supervised learning over histograms [20] and unsupervised learning of generative models [3]. For this simple case, the extension from probability distributions to arbitrary positive measures  $(\mu, \nu) \in \mathcal{M}_+(X)^2$  is now well understood and corresponds to the theory of unbalanced OT. Following [26, 12], a family of unbalanced Wasserstein distances is defined by solving

$$\text{UW}(\mu, \nu)^q \stackrel{\text{def.}}{=} \inf_{\pi \in \mathcal{M}(X \times X)} \int \lambda(d(x, y)) d\pi(x, y) + D_\varphi(\pi_1|\mu) + D_\varphi(\pi_2|\nu). \quad (2)$$

Here  $(\pi_1, \pi_2)$  are the two marginals of the joint distribution  $\pi$ , defined by  $\pi_1(A) = \pi(A \times Y)$  for  $A \subset X$ . The mapping  $\lambda : \mathbb{R}^+ \rightarrow \mathbb{R}$  and exponent  $q \geq 1$  should be chosen wisely to ensure for instance that UW defines a distance (see Section 2 for details).

It is frequent to take  $\rho D_\varphi$  instead of  $D_\varphi$  (or equivalently take  $\psi = \rho\varphi$ ) to adjust the strength of the penalization of the marginals. Classical (balanced) optimal transport is retrieved with  $\varphi = \iota_ =$  or by taking the limit  $\rho \rightarrow +\infty$ , which enforces exact conservation of mass  $\pi_1 = \mu$  and  $\pi_2 = \nu$ . In the limit  $\rho \rightarrow 0$ , when  $D_\varphi = \rho \text{KL}$  is the Kullback-Leibler relative entropy divergence,  $\text{UW}(\mu, \nu)^2/\rho$  tends to the squared Hellinger distance, which does not introduce any transportation at all. When  $0 < \rho < +\infty$ , unbalanced OT operates a tradeoff between transportation and creation of mass, which is crucial for instance to be robust to outliers in the data and to cope with mass variations in the modes of the distributions. For supervised tasks, the value of  $\rho$  should be cross-validated to obtain the best performances.

Its use is gaining popularity in applications, such as supervised learning [20], medical imaging registration [17], videos [25] and gradient flow to train neural

networks [9, 33]. Furthermore, existing efficient algorithms for balanced OT extend to this unbalanced problem. In particular Sinkhorn’s iterations, introduced in ML for balanced OT by [16], extend to unbalanced OT [11, 35], as detailed in Section 4.

**The Gromov-Wasserstein distance and its applications.** The Gromov-Wasserstein (GW) distance [28, 37] generalizes the notion of OT to the setting of mm-spaces up to isometries. It corresponds to replacing the linear cost  $\int \lambda(d) d\pi$  of OT by a quadratic function

$$\text{GW}(\mathcal{X}, \mathcal{Y})^q \stackrel{\text{def.}}{=} \min_{\pi \in \mathcal{M}_+(X \times Y)} \left\{ \int \lambda(\Gamma(x, x', y, y')) d\pi(x, y) d\pi(x', y') : \begin{array}{l} \pi_1 = \mu \\ \pi_2 = \nu \end{array} \right\}, \quad (3)$$

where the distortion kernel is  $\Gamma(x, x', y, y') \stackrel{\text{def.}}{=} \Delta(d_X(x, x'), d_Y(y, y'))$ , with  $\Delta$  any distance on  $\mathbb{R}_+$ . The construction detailed in [28, 37] considers  $\Delta$  the Euclidean distance,  $\lambda(r) = r^q$  with  $q \geq 1$ , in which case it is proved that GW defines a distance on balanced mm-spaces (i.e. the measures are probability distributions) up to isometries. In this paper, we extend this construction to the three cases of Section 2.2 and to arbitrary positive measures.

This distance is applied successfully in various domains. It is used in natural language processing for unsupervised translation learning [24, 1], in generative learning for objects lying in spaces of different dimensions [5] and to build VAE for graphs [43]. It has been adapted to take into consideration additional structures for domain adaptation over different spaces [31]. It is also a relevant distance to compute barycenters between graphs or shapes by leveraging additional features of the data [40] or the metric structure of GW [13]. In the specific case where the metric spaces are Euclidean, then this distance compares distributions up to rigid isometry, and is closely related (but not equal) to metrics defined by procrustes analysis [24, 2].

The problem (3) is non convex because the quadratic form  $\int \lambda(\Gamma) d\pi \otimes \pi$  is not positive in general. It is in fact closely related to quadratic assignment problems [7], which are used for graph matching problems, and are known to be NP-hard in general. Nevertheless, non-convex optimization methods have been shown to be successful in practice to use GW distances for ML problems. This includes for instance alternating minimization [28, 31] and entropic regularization [29, 22].

**Related works and contributions.** The work of [8] relaxes the GW distance to the unbalanced setting. It hybridizes GW with partial OT [19] for unsupervised labeling. It resembles one particular setting of our formulation, but with some important differences, detailed in Section 3. Our construction is also connected to partial matching methods, which find numerous applications in graphics and vision [14]. In particular, [32] introduces a mass conservation relaxation of the GW problem.

The two main contributions of this paper are the definition of two formulations relaxing the GW distance. The first one is called the Unbalanced Gromov-

Wasserstein (UGW) divergence and can be computed efficiently on GPUs. The second one is called the Conic Gromov-Wasserstein distance (CGW). It is proved to be a distance between mm-spaces endowed with positive measures up to isometries, as stated in Theorem 1 which is the main theoretical result of this paper. We also prove in Theorem 2 that UGW can be used as a surrogate upper-bounding CGW. We present those concepts and their properties in Section 3. We also detail in Section 4 an efficient computational scheme for a particular setting of UGW. This method computes an approximate stationary point of the non-convex energy. It leverages the strength of entropic regularization and the Sinkhorn algorithm, namely that it is GPU-friendly and defines smooth loss functions amenable to back-propagation for ML applications. Section 5 provides some numerical experiments to highlight the qualitative behavior of this algorithm, which shed some lights on the favorable properties of UGW to cope with outliers and mass variations in the modes of the distributions.

## 2 Background on unbalanced optimal transport

Following [26], this section reviews and generalizes the homogeneous and conic formulations of unbalanced optimal transport. These three formulations are equal in the convex setting of UOT. Our relaxed divergence UGW and conic distance CGW defined in Section 3 build upon those constructions but are not anymore equal due to the non-convexity of GW problems.

### 2.1 Homogeneous formulation

To ease the description of the homogeneous formulation, we use reverse Csiszàr entropy functions  $D_\psi$  defined below (1). Formulation (2) is rewritten as

$$\text{UW}(\mu, \nu)^q = \inf_{\pi \in \mathcal{M}(X^2)} \int L_{\lambda(d(x,y))}(f(x), g(y)) d\pi(x, y) + \psi'_\infty(|\mu^\perp| + |\nu^\perp|), \quad (4)$$

where  $L_c(r, s) \stackrel{\text{def.}}{=} c + \psi(r) + \psi(s)$ , with  $|\mu^\perp| \stackrel{\text{def.}}{=} \mu^\perp(X)$  and  $(f \stackrel{\text{def.}}{=} \frac{d\mu}{d\pi_1}, g \stackrel{\text{def.}}{=} \frac{d\nu}{d\pi_2})$  are the densities of the Lebesgue decomposition of  $(\mu, \nu)$  with respect to  $(\pi_1, \pi_2)$  and

$$\mu = f\pi_1 + \mu^\perp \quad \text{and} \quad \nu = g\pi_2 + \nu^\perp. \quad (5)$$

Reverse entropies are helpful to explicit the terms of pure mass creation/destruction  $(|\mu^\perp| + |\nu^\perp|)$  and reinterpret the integral under  $\pi$  as a transport term with a new cost  $L_{\lambda(d)}$ .

Then the authors of [26] define the homogeneous formulations HUW as

$$\text{HUW}(\mu, \nu)^q \stackrel{\text{def.}}{=} \inf_{\pi \in \mathcal{M}(X^2)} \int H_{\lambda(d(x,y))}(f(x), g(y)) d\pi(x, y) + \psi'_\infty(|\mu^\perp| + |\nu^\perp|), \quad (6)$$

where the 1-homogeneous function  $H_c$  is the perspective transform of  $L_c$

$$H_c(r, s) \stackrel{\text{def.}}{=} \inf_{\theta \geq 0} \theta \left( c + \psi\left(\frac{r}{\theta}\right) + \psi\left(\frac{s}{\theta}\right) \right) = \inf_{\theta \geq 0} \theta L_c\left(\frac{r}{\theta}, \frac{s}{\theta}\right). \quad (7)$$

By definition one has  $L_c \geq H_c$ , thus  $UW \geq HUW$ . In fact, one actually has  $UW = HUW$  as proved in [26, Theorem 5.8].

## 2.2 Cone sets, cone distances and explicit settings

The conic formulation detailed in Section 2.3 is obtained by performing the optimal transport on the cone set  $\mathfrak{C}[X] \stackrel{\text{def.}}{=} X \times \mathbb{R}_+ / (X \times \{0\})$ , where the extra coordinate accounts for the mass of the particle. Coordinates of the form  $(x, 0)$  are merged into a single point called the apex of the cone, noted  $\mathfrak{o}_X$ . In the sequel, points of  $X \times \mathbb{R}_+$  are noted  $(x, r)$  and those of  $\mathfrak{C}[X]$  are noted  $[x, r]$  to emphasize the quotient operation at the apex.

For a pair  $(p, q) \in \mathbb{R}_+$ , we define for any  $[x, r], [y, s] \in \mathfrak{C}[X]^2$

$$\mathcal{D}_{\mathfrak{C}[X]}([x, r], [y, s])^q \stackrel{\text{def.}}{=} H_{\lambda(d(x, y))}(r^p, s^p). \quad (8)$$

In general  $\mathcal{D}_{\mathfrak{C}[X]}$  is not a distance, but it is always definite as proved by the following result.

**Proposition 1.** *Assume that  $d$  is definite,  $\lambda^{-1}(\{0\}) = \{0\}$  and  $\varphi^{-1}(\{0\}) = \{1\}$ . Assume also that for any  $(r, s)$ , there always exists  $\theta^*$  such that  $H_c(r, s) = \theta^* L_c(\frac{r}{\theta^*}, \frac{s}{\theta^*})$ .*

*Then  $\mathcal{D}_{\mathfrak{C}[X]}$  is definite on  $\mathfrak{C}[X]$ , i.e.  $\mathcal{D}_{\mathfrak{C}[X]}([x, r], [y, s]) = 0$  if and only if  $(r = s = 0)$  or  $(r = s \text{ and } x = y)$ .*

*Proof.* Assume  $\mathcal{D}_{\mathfrak{C}[X]}([x, r], [y, s]) = 0$ , and write  $\theta^*$  such that

$$\begin{aligned} \mathcal{D}_{\mathfrak{C}[X]}([x, r], [y, s])^q &= \theta^* L_c(\frac{r^p}{\theta^*}, \frac{s^p}{\theta^*}) \\ &= \theta^* \lambda(d(x, y)) + r^p \varphi(\frac{\theta^*}{r^p}) + s^p \varphi(\frac{\theta^*}{s^p}), \end{aligned}$$

where the last line is given by the definition of reverse entropy.

There are two cases. If  $\theta^* > 0$ , since all terms are positive, there are all equal to 0. By definiteness of  $d$  it yields  $x = y$  and because  $\varphi^{-1}(\{0\}) = \{1\}$  we have  $r^p = s^p = \theta^*$  and  $r = s$ . If  $\theta^* = 0$  then  $\mathcal{D}_{\mathfrak{C}[X]}([x, r], [y, s])^q = \varphi(0)(r^p + s^p)$ . The assumption  $\varphi^{-1}(\{0\}) = \{1\}$  implies  $\varphi(0) > 0$ , thus necessarily  $r = s = 0$ .  $\square$

The function  $H_c$  can be computed in closed form for a certain number of common entropies  $\varphi$ , and we refer to [26, Section 5] for an overview. Of particular interest are those  $\varphi$  where  $\mathcal{D}_{\mathfrak{C}[X]}$  is a distance, which necessitates a careful choice of  $\lambda, p$  and  $q$ . We now detail three particular settings where this is the case. In each setting we provide  $(D_\varphi, \lambda, p, q)$  and its associated cone distance  $\mathcal{D}_{\mathfrak{C}[X]}$ .

**Gaussian Hellinger distance** It corresponds to

$$\begin{aligned} D_\varphi &= \text{KL}, \quad \lambda(t) = t^2 \quad \text{and} \quad q = p = 2, \\ \mathcal{D}_{\mathfrak{C}[X]}([x, r], [y, s])^2 &= r^2 + s^2 - 2rs e^{-d(x, y)/2}, \end{aligned}$$

in which case it is proved in [26] that  $\mathcal{D}_{\mathfrak{C}[X]}$  is a cone distance.

**Hellinger-Kantorovich / Wasserstein-Fisher-Rao distance** It reads

$$\begin{aligned} D_\varphi &= \text{KL}, \quad \lambda(t) = -\log \cos^2(t \wedge \frac{\pi}{2}) \quad \text{and} \quad q = p = 2, \\ \mathcal{D}_{\mathfrak{C}[X]}([x, r], [y, s])^2 &= r^2 + s^2 - 2rs \cos(\frac{\pi}{2} \wedge d(x, y)), \end{aligned}$$

in which case it is proved in [6] that  $\mathcal{D}_{\mathfrak{C}[X]}$  is a cone distance.

The weight  $\lambda(t) = -\log \cos^2(t \wedge \frac{\pi}{2})$ , which might seem more peculiar, is in fact the penalty that makes unbalanced OT a length space induced by the Gaussian-Hellinger distance (if the ground metric  $d$  is itself geodesic), as proved in [27, 10]. This weight introduces a cut-off, because  $\lambda(d(x, y)) = +\infty$  if  $d(x, y) > \pi/2$ . There is no transport between points too far from each other. The choice of  $\pi/2$  is arbitrary, and can be modified by scaling  $\lambda \mapsto \lambda(\cdot/s)$  for some cutoff  $s$ .

**Partial optimal transport** It corresponds to

$$\begin{aligned} D_\varphi &= \text{TV}, \quad \lambda(t) = t^q \quad \text{and} \quad q \geq 1 \quad \text{and} \quad p = 1, \\ \mathcal{D}_{\mathfrak{C}[X]}([x, r], [y, s])^q &= r + s - (r \wedge s)(2 - d(x, y)^q)_+, \end{aligned}$$

in which case it is proved in [12] that  $\mathcal{D}_{\mathfrak{C}[X]}$  is a cone distance. The case  $D_\varphi = \text{TV}$  is equivalent to partial unbalanced OT, which produces discontinuities (because of the non-smoothness of the divergence) between regions of the supports which are being transported and regions where mass is being destroyed/created.

Note that [26] do not mention that this  $\mathcal{D}_{\mathfrak{C}[X]}$  defines a distance, so this result is new to the best of our knowledge, although it can be proved without a conic lifting that partial OT defines a distance as explained in [12].

### 2.3 Conic formulation of UW

The last formulation reinterprets HUW as an OT problem on the cone, with the addition of two linear constraints. Informally speaking,  $H_c$  becomes  $\mathcal{D}_{\mathfrak{C}[X]}$ , the term  $(|\mu^\perp| + |\nu^\perp|)$  is taken into account by the constraints (10) below, and the variables  $(f, g)$  are replaced by  $(r^p, s^p)$ . It reads

$$\text{CUW}(\mu, \nu)^q \stackrel{\text{def.}}{=} \inf_{\alpha \in \mathcal{U}_p(\mu, \nu)} \int \mathcal{D}_{\mathfrak{C}[X]}([x, r], [y, s])^q d\alpha([x, r], [y, s]), \quad (9)$$

where the constraint set  $\mathcal{U}_p(\mu, \nu)$  is defined as

$$\mathcal{U}_p(\mu, \nu) \stackrel{\text{def.}}{=} \left\{ \alpha \in \mathcal{M}_+(\mathfrak{C}[X]^2) : \int_{\mathbb{R}_+} r^p d\alpha_1(\cdot, r) = \mu, \int_{\mathbb{R}_+} s^p d\alpha_2(\cdot, s) = \nu \right\}. \quad (10)$$

Thus CUW consists in minimizing the Wasserstein distance  $W_{\mathcal{D}_{\mathfrak{C}[X]}}(\alpha_1, \alpha_2)$  on the cone  $(\mathfrak{C}[X], \mathcal{D}_{\mathfrak{C}[X]})$ . The additional constraints on  $(\alpha_1, \alpha_2)$  mean that the lift of the mass on the cone must be consistent with the total mass of  $(\mu, \nu)$ .

When  $\mathcal{D}_{\mathfrak{C}[X]}$  is a distance, CUW inherits the metric properties of  $W_{\mathcal{D}_{\mathfrak{C}[X]}}$ . Our theoretical results rely on an analog construction for GW.

The following proposition states the equality of the three formulations and recapitulates its main properties.

**Proposition 2** (From [26]). *One has  $UW = HUW = CUW$ , which are symmetric, positive and definite. Furthermore, if  $(X, d_X)$  and  $(\mathfrak{C}[X], \mathcal{D}_{\mathfrak{C}[X]})$  are metric spaces with  $X$  separable, then  $\mathcal{M}_+(X)$  endowed with CUW is a metric space.*

*Proof.* The equality  $UW = HUW$  is given by [26, Theorem 5.8], while the equality  $HUW = CUW$  holds thanks to [26, Theorem 6.7 and Remark 7.5], where the latter theorem can be straightforwardly generalized to any cone distance defined by (8). Since  $\mathcal{D}_{\mathfrak{C}[X]}$  is symmetric, positive and definite (see Proposition 1), then so is CUW. Furthermore, if  $\mathcal{D}_{\mathfrak{C}[X]}$  satisfies the triangle inequality, separability of  $X$  allows to apply the gluing lemma [26, Corollary 7.14] which generalizes to any exponent  $p$  defining  $\mathcal{U}_p(\mu, \nu)$  and any cone distance  $\mathcal{D}_{\mathfrak{C}[X]}$ .  $\square$

### 3 Unbalanced Gromov-Wasserstein formulations

We present in this section our two new formulations and their properties. The first one, called UGW, is amenable to computation on GPUs, and is exploited in Section 4 to derive an efficient algorithm, which is used in the numerical experiments of Section 5. The second one, called CGW, defines a distance between mm-spaces up to isometries.

In all what follows, we consider complete separable mm-spaces endowed with a metric and a positive measure.

#### 3.1 The unbalanced Gromov-Wasserstein divergence

This new formulation makes use of quadratic  $\varphi$ -divergences, defined as  $D_\varphi^\otimes(\rho|\nu) \stackrel{\text{def.}}{=} D_\varphi(\rho \otimes \rho | \nu \otimes \nu)$ , where  $\rho \otimes \rho \in \mathcal{M}_+(X^2)$  is the tensor product measure defined by  $d(\rho \otimes \rho)(x, y) = d\rho(x)d\rho(y)$ . Note that  $D_\varphi^\otimes$  is not a convex function in general.

**Definition 1** (Unbalanced GW). *The Unbalanced Gromov-Wasserstein divergence is defined as*

$$\begin{aligned} \text{UGW}(\mathcal{X}, \mathcal{Y}) &= \inf_{\pi \in \mathcal{M}^+(X \times Y)} \mathcal{L}(\pi) \quad \text{where} \\ \mathcal{L}(\pi) &\stackrel{\text{def.}}{=} \int_{X^2 \times Y^2} \lambda(\Gamma(x, x', y, y')) d\pi(x, y) d\pi(x', y') + D_\varphi^\otimes(\pi_1 | \mu) + D_\varphi^\otimes(\pi_2 | \nu). \end{aligned} \tag{11}$$

This definition can be understood as an hybridation between (3) and (2) but with a twist: one needs to use the quadratic divergence  $D_\varphi^\otimes$  in place of  $D_\varphi$ . In the TV case, this is the most important distinction between UGW and partial GW [8]. Using quadratic divergences results in UGW being 2-homogeneous: if  $\mu$  and  $\nu$  are multiplied by  $\theta \geq 0$ , then  $\text{UGW}(\mathcal{X}, \mathcal{Y})$  is multiplied by  $\theta^2$ . Not



using such divergences results in a lack of 2-homogeneity of  $\mathcal{L}$  which is crucial to show the connection between our proposed formulations. Note also that the balanced GW distance (3) is recovered as a particular case when using  $\varphi = \iota_-$  or by letting  $\rho \rightarrow +\infty$  for an entropy  $\psi = \rho\varphi$ .

We first prove the existence of optimal plans  $\pi$  solution to (11). The hypotheses of this theorem cover the three key settings of Section 2.2. This proposition is proved in Appendix C.

**Proposition 3** (Existence of minimizers). *We assume that  $(X, Y)$  are compact and that either (i)  $\varphi$  superlinear, i.e  $\varphi'_\infty = \infty$ , or (ii)  $\lambda$  has compact sublevel sets in  $\mathbb{R}_+$  and  $2\varphi'_\infty + \inf \lambda > 0$ . Then there exists  $\pi \in \mathcal{M}_+(X \times Y)$  such that  $\text{UGW}(\mathcal{X}, \mathcal{Y}) = \mathcal{L}(\pi)$ .*

The following proposition ensures that the functional UGW can be used to compare mm-spaces.

**Proposition 4.** *Assume that  $\varphi^{-1}(\{0\}) = \{1\}$  and  $\lambda^{-1}(\{0\}) = \{0\}$ . Then  $\text{UGW}(\mathcal{X}, \mathcal{Y}) \geq 0$  and is 0 if and only if  $\mathcal{X} \sim \mathcal{Y}$ .*

*Proof.* Assume  $\text{UGW}(\mathcal{X}, \mathcal{Y}) = 0$ . In the three considered settings, positivity implies that all the terms appearing in  $\mathcal{L}$  are zero. Similarly to the balanced case [28], the distortion being zero imposes that the plan  $\pi$  defines an isometry. The  $\varphi$ -divergences being zero implies that  $\pi$  has marginals equal to  $(\mu, \nu)$ . This plan thus defines an isometric bijection between  $\mathcal{X}$  and  $\mathcal{Y}$ , see Appendix B for details.  $\square$

We end this section with a lemma which makes an analogy with Equation (4), and makes the transition with the next section on the conic formulation. Its proof is deferred to Appendix B.

**Lemma 1.** *One has*

$$\mathcal{L}(\pi) = \int_{X^2 \times Y^2} L_{\lambda(\Gamma)}(f \otimes f, g \otimes g) d\pi d\pi + \psi'_\infty(|(\mu \otimes \mu)^\perp| + |(\nu \otimes \nu)^\perp|), \quad (12)$$

where  $(f, g)$  are given by (5).

## 3.2 The conic Gromov-Wasserstein distance

We introduce a second conic-GW formulation adapted from (9) which is connected to UGW. Most importantly is Theorem 1 which states that it defines a distance between mm-spaces equipped with arbitrary positive measures.

### 3.2.1 Conic formulation

We refer to Section 2 for the construction of cone sets. We consider the cone distance  $\mathcal{D} \stackrel{\text{def}}{=} \mathcal{D}_{\mathfrak{C}[\mathbb{R}_+]}$  on  $\mathbb{R}$ , where the distance  $d$  of (8) is now  $\Delta$  from (3). The conic formulations optimizes over measures  $\alpha \in \mathcal{U}_p(\mu, \nu)$  defined in Equation (10),

with the slight change that  $\alpha \in \mathcal{M}_+(\mathfrak{C}[X] \times \mathfrak{C}[Y])$  instead of  $\mathcal{M}_+(\mathfrak{C}[X]^2)$  for UW (9). It reads  $\text{CGW}(\mathcal{X}, \mathcal{Y}) \stackrel{\text{def.}}{=} \inf_{\alpha \in \mathcal{U}_p(\mu, \nu)} \mathcal{H}(\alpha)$  where

$$\mathcal{H}(\alpha) \stackrel{\text{def.}}{=} \int \mathcal{D}([d_X(x, x'), rr'], [d_Y(y, y'), ss'])^q d\alpha([x, r], [y, s]) d\alpha([x', r'], [y', s']). \quad (13)$$

It is an adaptation of the program (9) to GW. Starting from Lemma 1, we perform a derivation similar to the construction of CUW from UW as presented in Section 2. The densities  $f(x), f(x'), g(y), g(y')$  are replaced by variables  $r^p, r'^p, s^p, s'^p$ , and the tensor structure  $r \cdot r'$  of those variables is due to the tensorized structure of the plan  $\alpha \otimes \alpha$ .

Note that similarly to the GW formulation (3) – and in sharp contrast with the formulation (9) of UW – here the transport plans are defined on the cone  $\mathfrak{C}[X] \times \mathfrak{C}[Y]$  but the cost  $\mathcal{D}$  is a distance on  $\mathfrak{C}[\mathbb{R}_+]$ .

We state that CGW defines a distance in the theorem below.

**Theorem 1.** *The divergence CGW is symmetric, positive and definite up to isometries. Furthermore, if  $\mathcal{D}$  is a distance on  $\mathfrak{C}[\mathbb{R}_+]$ , then  $\text{CGW}^{1/q}$  is a distance on the set of mm-spaces up to isometries.*

As an application of the above result we have the following corollary.

**Corollary 1.** *When  $\Delta$  is the Euclidean distance on  $\mathbb{R}$ , for all choices of  $(D_\varphi, \lambda, p, q)$  given in Section 2.2,  $\text{CGW}^{1/q}$  is a distance on the set of mm-spaces up to isometries.*

The next theorem shows that while the distance  $\text{CGW}^{1/q}$  seems difficult to compute (because it is defined on a lifted space), it can be controlled by UGW, which can be approximated with efficient numerical schemes as detailed in Section 4.

**Theorem 2.** *For any choice of  $(D_\varphi, \lambda, p, q)$  and for  $\mathcal{D}$  defined with Equation (8), one has  $\text{UGW} \geq \text{CGW}$ .*

### 3.2.2 Preliminary results

We present concepts and properties which are necessary for the proofs of Theorem 1 and Theorem 2.

**Definition 2** (dilations). *Consider  $v([x, r], [y, s])$  a Borel measurable scaling function depending on  $[x, r], [y, s] \in \mathfrak{C}[X] \times \mathfrak{C}[Y]$ . Take a plan  $\alpha \in \mathcal{M}_+(\mathfrak{C}[X] \times \mathfrak{C}[Y])$ . We define the dilation  $\text{Dil}_v : \alpha \mapsto (h_v)_\#(v^p \alpha)$  where*

$$h_v([x, r], [y, s]) \stackrel{\text{def.}}{=} ([x, r/w], [y, s/w]),$$

where  $w = v([x, r], [y, s])$ . It reads for any test function  $\xi$

$$\int \xi([x, r], [y, s]) d\text{Dil}_v(\alpha) = \int \xi([x, r/w], [y, s/w]) w^p d\alpha.$$

A crucial property of the conic formulation (13) is its invariance to dilations of the radial coordinates. We state this invariance in the following lemma. The proof can be found in Appendix C.

**Lemma 2** (Invariance to dilation). *The problem CGW is invariant to dilations, i.e. for any  $\alpha \in \mathcal{U}_p(\mu, \nu)$ , we have  $\text{Dil}_v(\alpha) \in \mathcal{U}_p(\mu, \nu)$  and  $\mathcal{H}(\alpha) = \mathcal{H}(\text{Dil}_v(\alpha))$ .*

The invariance to dilation allows one to normalize the plan  $\alpha$  and assume extra properties without loss of generality. For instance with  $v = \alpha(\mathfrak{C}[X] \times \mathfrak{C}[Y])^{-1/q}$  we can assume that  $\alpha$  is a probability distribution, which allows us to leverage results of balanced optimal transport on the cone. It can also be leveraged to prove the following lemma, which is used to prove the triangle inequality.

**Lemma 3** (Normalization lemma). *Assume there exists  $\alpha \in \mathcal{U}_p(\mu, \nu)$  s.t.  $\text{CGW}(\mathcal{X}, \mathcal{Y}) = \mathcal{H}(\alpha)$ . Then there exists  $\tilde{\alpha}$  such that  $\tilde{\alpha} \in \mathcal{U}_p(\mu, \nu)$ ,  $\text{CGW}(\mathcal{X}, \mathcal{Y}) = \mathcal{H}(\tilde{\alpha})$  and whose marginal on  $\mathfrak{C}[Y]$  is*

$$\nu_{\mathfrak{C}[Y]} = \delta_{\mathbf{o}_Y} + \mathbf{p}_{\#}(\nu \otimes \delta_1),$$

where  $\mathbf{p} : X \times \mathbb{R}_+ \rightarrow \mathfrak{C}[X]$  is the canonical injection into the cone that reads  $\mathbf{p}(x, r) \stackrel{\text{def}}{=} [x, r]$ .

Before detailing the computational algorithm in Section 4, we provide the proofs of our main results.

### 3.2.3 Proof of Theorem 1

*Non-negativity* and *symmetry* hold since  $\mathcal{H}$  is a sum of non-negative symmetric terms. To prove *Definiteness*, assume  $\text{CGW}(\mathcal{X}, \mathcal{Y}) = 0$ , and write  $\alpha$  an optimal plan. We have  $\alpha \otimes \alpha$ -a.e. that  $d_X(x, x') = d_Y(y, y')$  and  $rr' = ss'$  because  $\mathcal{D}$  is definite (see Proposition 1). Thanks to the completeness of  $(\mathcal{X}, \mathcal{Y})$  and a result from [37, Lemma 1.10], such property implies the existence of a Borel isometric bijection with Borel inverse between the supports of the measures  $\psi : \text{Supp}(\mu) \rightarrow \text{Supp}(\nu)$ , where  $\text{Supp}$  denotes the support. The bijection  $\psi$  verifies  $d_X(x, x') = d_Y(\psi(x), \psi(x'))$ . To prove  $\mathcal{X} \sim \mathcal{Y}$  it remains to prove  $\psi_{\#}\mu = \nu$ . Due to the density of continuous functions of the form  $\xi(x)\xi(x')$ , the constraints of  $\mathcal{U}_p(\mu, \nu)$  are equivalent to

$$\int_{\mathbb{R}_+} (rr')^p d\alpha_1(\cdot, r) d\alpha_1(\cdot, r') = \mu \otimes \mu, \quad \int_{\mathbb{R}_+} (ss')^p d\alpha_2(\cdot, s) d\alpha_2(\cdot, s') = \nu \otimes \nu.$$

Take a continuous test function  $\xi$  defined on  $\text{Supp}(\nu)^2$ . Writing  $y = \psi(x)$  and  $y' = \psi(x')$ , one has

$$\begin{aligned} \int \xi(y, y') d\nu d\nu &= \int \xi(y, y') (ss')^p d\alpha d\alpha \\ &= \int \xi(\psi(x), \psi(x')) (ss')^p d\alpha d\alpha \\ &= \int \xi(\psi(x), \psi(x')) (rr')^p d\alpha d\alpha \end{aligned}$$

$$\begin{aligned}
\int \xi(y, y') d\nu d\nu &= \int \xi(\psi(x), \psi(x')) d\mu d\mu \\
&= \int \tilde{\xi}(x, x') d\psi_{\#}\mu d\psi_{\#}\mu.
\end{aligned}$$

Since  $\psi$  is a bijection, there is a bijection between continuous functions  $\xi$  of  $\text{Supp}(\nu)^2$  and functions  $\tilde{\xi}$  of  $\text{Supp}(\mu)^2$ . Thus we obtain  $\nu = \psi_{\#}\mu$  and we have  $\mathcal{X} \sim \mathcal{Y}$ .

It remains to prove the *triangle inequality*. Assume now that  $\mathcal{D}$  satisfies it. Given three mm-spaces  $(\mathcal{X}, \mathcal{Y}, \mathcal{Z})$  respectively equipped with measures  $(\mu, \nu, \eta)$ , consider  $\alpha, \beta$  which are optimal plans for  $\text{CGW}(\mathcal{X}, \mathcal{Y})$  and  $\text{CGW}(\mathcal{Y}, \mathcal{Z})$ . Using Lemma 3 to both  $\alpha$  and  $\beta$ , we can consider measures  $(\bar{\alpha}, \bar{\beta})$  which are also optimal and have a common marginal  $\bar{\nu}$  on  $\mathfrak{C}[Y]$ . Thanks to this common marginal and the separability of  $(X, Y, Z)$ , the standard gluing lemma [41, Lemma 7.6] applies and yields a glued plan  $\gamma \in \mathcal{M}_+(\mathfrak{C}[X] \times \mathfrak{C}[Y] \times \mathfrak{C}[Z])$  whose respective marginals on  $\mathfrak{C}[X] \times \mathfrak{C}[Y]$  and  $\mathfrak{C}[Y] \times \mathfrak{C}[Z]$  are  $(\bar{\alpha}, \bar{\beta})$ . Furthermore, the marginal  $\bar{\gamma}$  of  $\gamma$  on  $\mathfrak{C}[X] \times \mathfrak{C}[Z]$  is in  $\mathcal{U}_p(\mu, \eta)$ . Indeed,  $(\bar{\gamma}, \bar{\alpha})$  have the same marginal on  $\mathfrak{C}[X]$  and same for  $(\bar{\gamma}, \bar{\beta})$  on  $\mathfrak{C}[Z]$ , hence this property. Write  $d_X = d_X(x, x')$  for sake of conciseness (and similarly for  $Y, Z$ ). The calculation reads

$$\text{CGW}(\mathcal{X}, \mathcal{Z})^{\frac{1}{q}} \quad (14)$$

$$\leq \left( \int \mathcal{D}([d_X, rr'], [d_Z, tt'])^q d\bar{\gamma}([x, r], [z, t]) d\bar{\gamma}([x', r'], [z', t']) \right)^{\frac{1}{q}} \quad (15)$$

$$\leq \left( \int \mathcal{D}([d_X, rr'], [d_Z, tt'])^q d\gamma([x, r], [y, s], [z, t]) d\gamma([x', r'], [y', s'], [z', t']) \right)^{\frac{1}{q}} \quad (16)$$

$$\leq \left( \int (\mathcal{D}([d_X, rr'], [d_Y, ss']) + \mathcal{D}([d_Y, ss'], [d_Z, tt']))^q d\gamma d\gamma \right)^{\frac{1}{q}} \quad (17)$$

$$\leq \left( \int \mathcal{D}([d_X, rr'], [d_Y, ss'])^q d\gamma d\gamma \right)^{\frac{1}{q}} + \left( \int \mathcal{D}([d_Y, ss'], [d_Z, tt'])^q d\gamma d\gamma \right)^{\frac{1}{q}} \quad (18)$$

$$\begin{aligned}
&\leq \left( \int \mathcal{D}([d_X, rr'], [d_Y, ss'])^q d\bar{\alpha}([x, r], [y, s]) d\bar{\alpha}([x', r'], [y', s']) \right)^{\frac{1}{q}} \\
&\quad + \left( \int \mathcal{D}([d_Y, ss'], [d_Z, tt'])^q d\bar{\beta}([y, s], [z, t]) d\bar{\beta}([y', s'], [z', t']) \right)^{\frac{1}{q}} \quad (19)
\end{aligned}$$

$$\leq \text{CGW}(\mathcal{X}, \mathcal{Y})^{\frac{1}{q}} + \text{CGW}(\mathcal{Y}, \mathcal{Z})^{\frac{1}{q}}. \quad (20)$$

Since  $\bar{\gamma} \in \mathcal{U}_p(\mu, \eta)$ , it is thus suboptimal, which yields Equation (15). Because  $\bar{\gamma}$  is the marginal of  $\gamma$  we get Equation (16). Equations (17) and (18) are respectively obtained by the triangle and Minkowski inequalities, which hold because  $\mathcal{D}$  which is a distance. Equation (19) is the marginalization of  $\gamma$ , and Equation (20) is given by the optimality of  $(\bar{\alpha}, \bar{\beta})$ , which ends the proof of the triangle inequality.

### 3.2.4 Proof of Theorem 2

The proof consists in considering an optimal plan  $\pi$  for UGW, building a lift  $\alpha$  of this plan into the cone such that  $\mathcal{L}(\pi) \geq \mathcal{H}(\alpha)$ , and prove that  $\alpha$  is admissible for the program CGW, thus suboptimal.

Using Equation (5), we have

$$\begin{aligned}\mu \otimes \mu &= (f \otimes f)\pi_1 \otimes \pi_1 + (\mu \otimes \mu)^\perp, \\ (\mu \otimes \mu)^\perp &= \mu^\perp \otimes (f\pi_1) + (f\pi_1) \otimes \mu^\perp + \mu^\perp \otimes \mu^\perp, \\ \nu \otimes \nu &= (g \otimes g)\pi_2 \otimes \pi_2 + (\nu \otimes \nu)^\perp, \\ (\nu \otimes \nu)^\perp &= \nu^\perp \otimes (g\pi_2) + (g\pi_2) \otimes \nu^\perp + \nu^\perp \otimes \nu^\perp.\end{aligned}\tag{21}$$

Recall that the canonic injection  $\mathbf{p}$  reads  $\mathbf{p}(x, r) = [x, r]$ . Based on the above Lebesgue decomposition, we define the conic plan

$$\alpha = (\mathbf{p}(x, f(x)^{\frac{1}{p}}), \mathbf{p}(y, g(y)^{\frac{1}{p}}))_\# \pi(x, y) + \delta_{\mathbf{o}_X} \otimes \mathbf{p}_\#[\nu^\perp \otimes \delta_1] + \mathbf{p}_\#[\mu^\perp \otimes \delta_1] \otimes \delta_{\mathbf{o}_Y}.\tag{22}$$

We have that  $\alpha \in \mathcal{U}_p(\mu, \nu)$ . Indeed for the first marginal (and similarly for the second) we have for any test function  $\xi(x)$

$$\begin{aligned}\int \xi(x)(r)^p d\alpha &= \int \xi(x)f(x)d\pi_1(x) + 0 + \int \xi(x)(1)^p d\mu^\perp(x) \\ &= \int \xi(x)d(f(x)\pi_1 + \mu^\perp) \\ &= \int \xi(x)d\mu(x).\end{aligned}$$

We define  $\theta^* = \theta_c^*(r, s)$  the parameter which verifies  $H_c(r, s) = \theta^* L_c(r/\theta^*, s/\theta^*)$ . We restrict  $\alpha \otimes \alpha$  to the set  $S = \{\theta_{\lambda(\Gamma)}^*((rr')^p, (ss')^p) > 0\}$ . By construction,  $\theta_c^*(r, s)$  is 1-homogeneous in  $(r, s)$ . Thus on  $S$  we necessarily have  $r, r', s, s' > 0$ . It yields

$$\alpha \otimes \alpha|_S = (\mathbf{p}(x, f(x)^{\frac{1}{p}}), \mathbf{p}(y, g(y)^{\frac{1}{p}}), \mathbf{p}(x', f(x')^{\frac{1}{p}}), \mathbf{p}(y', g(y')^{\frac{1}{p}}))_\# (\pi \otimes \pi).$$

Concerning the orthogonal part of the decomposition, note that whenever  $\theta^* = 0$ , due to the definition of  $H$  the cone distance reads

$$\mathcal{D}([x, r], [y, s])^q = \psi'_\infty(r^p + s^p).\tag{23}$$

It geometrically means that the shortest path between  $[x, r]$  and  $[y, s]$  must pass via the apex, which corresponds to a pure mass creation/destruction regime.

Furthermore we have that

$$\begin{aligned}|(\mu \otimes \mu)^\perp| &= \int (r \cdot r')^p d(\alpha \otimes \alpha)|_{S^c}, \\ |(\nu \otimes \nu)^\perp| &= \int (s \cdot s')^p d(\alpha \otimes \alpha)|_{S^c}.\end{aligned}$$

Indeed, thanks to Equation (22) we have for the first marginal that

$$\begin{aligned}
|(\mu \otimes \mu)^\perp| &= (\mu^\perp \otimes (f\pi_1) + (f\pi_1) \otimes \mu^\perp + \mu^\perp \otimes \mu^\perp)(X^2) \\
&= \int (rr')^p d\mathbf{p}_\#[\mu^\perp \otimes \delta_1] d\mathbf{p}(x', f(x')^{\frac{1}{p}})_\# \pi_1(x') \\
&\quad + \int (rr')^p d\mathbf{p}(x, f(x)^{\frac{1}{p}})_\# \pi_1(x) d\mathbf{p}_\#[\mu^\perp \otimes \delta_1] \\
&\quad + \int (rr')^p d\mathbf{p}_\#[\mu^\perp \otimes \delta_1] d\mathbf{p}_\#[\mu^\perp \otimes \delta_1] \\
&= \int (rr')^p d(\alpha \otimes \alpha)|_{S^c}.
\end{aligned}$$

Note that the last equality holds because each term of  $\alpha \otimes \alpha$  involving a measure  $\delta_{\mathbf{o}_X}$  cancels out when integrated against  $(rr')^p$ .

Eventually the computation gives (thanks to Lemma 1)

$$\begin{aligned}
\mathcal{L}(\pi) &= \int_{X^2 \times Y^2} L_{\lambda(\Gamma)}(f \otimes f, g \otimes g) d\pi d\pi + \psi'_\infty(|(\mu \otimes \mu)^\perp| + |(\nu \otimes \nu)^\perp|) \\
&\geq \int H_{\lambda(\Gamma)}(f \otimes f, g \otimes g) d\pi d\pi + \psi'_\infty(|(\mu \otimes \mu)^\perp| + |(\nu \otimes \nu)^\perp|) \\
&\geq \int \mathcal{D}([d_X(x, x'), (f \otimes f)^{\frac{1}{p}}], [d_Y(y, y'), (g \otimes g)^{\frac{1}{p}}])^q d\pi d\pi \\
&\quad + \int \psi'_\infty(rr')^p d(\alpha \otimes \alpha)|_{S^c} + \int \psi'_\infty(ss')^p d(\alpha \otimes \alpha)|_{S^c} \\
&\geq \int \mathcal{D}([d_X(x, x'), rr'], [d_Y(y, y'), ss'])^q d(\alpha \otimes \alpha)|_S \\
&\quad + \int \psi'_\infty((rr')^p + (ss')^p) d(\alpha \otimes \alpha)|_{S^c} \\
&\geq \int \mathcal{D}([d_X(x, x'), rr'], [d_Y(y, y'), ss'])^q d\alpha d\alpha \\
&\geq \mathcal{H}(\alpha).
\end{aligned}$$

Thus we have  $\text{UGW}(\mathcal{X}, \mathcal{Y}) = \mathcal{L}(\pi) \geq \mathcal{H}(\alpha) \geq \text{CGW}(\mathcal{X}, \mathcal{Y})$ .

## 4 Algorithms

The computation of the distance CGW is in practice out-of-reach because it requires an optimization over a lifted conic space, which would need to be discretized. We focus in this section on the numerical computation of the upper bound UGW, using an alternate minimization coupled with entropic regularization. The algorithm is presented on arbitrary measures, the special case of discrete measures being a particular case. The discretized formulas are detailed in Appendix A, see also [11, 29]. All implementations are available at [https://github.com/thibsej/unbalanced\\_gromov\\_wasserstein](https://github.com/thibsej/unbalanced_gromov_wasserstein).

In order to derive a simple numerical approximation scheme, following [28], we introduce a lower bound obtained by introducing two transportation plans. To further accelerate the method and enable GPU-friendly iterations, similarly to [23, 36], we consider an entropic regularization. It reads, for any  $\varepsilon \geq 0$ ,

$$\begin{aligned} \text{UGW}_\varepsilon(\mathcal{X}, \mathcal{Y}) &\stackrel{\text{def.}}{=} \inf_{\pi} \mathcal{L}(\pi) + \varepsilon \text{KL}^\otimes(\pi | \mu \otimes \nu) \\ &\geq \inf_{\pi, \gamma} \mathcal{F}(\pi, \gamma) + \varepsilon \text{KL}(\pi \otimes \gamma | (\mu \otimes \nu)^{\otimes 2}), \end{aligned} \quad (24)$$

$$\text{where } \mathcal{F}(\pi, \gamma) \stackrel{\text{def.}}{=} \int_{X^2 \times Y^2} \lambda(\Gamma) d\pi \otimes \gamma + D_\varphi(\pi_1 \otimes \gamma_1 | \mu \otimes \mu) + D_\varphi(\pi_2 \otimes \gamma_2 | \nu \otimes \nu).$$

Note that in contrast to the entropic regularization of GW [29], here we use a tensorized entropy to maintain the overall homogeneity of the energy. A simple method to approximate this lower bound is to perform an alternate minimization on  $\pi$  and  $\gamma$ , which is known to converge for smooth  $\varphi$  to a stationary point since the coupling term in the functional is smooth [39].

Note that if  $\pi \otimes \gamma$  is optimal then so is  $(s\pi) \otimes (\frac{1}{s}\gamma)$  with  $s \geq 0$ . Thus without loss of generality we optimize under the constraint  $m(\pi) = m(\gamma)$ . In general, this bound is not expected to be tight, but empirically, alternate minimization often converges to a solution with  $\pi = \gamma$  (as already observed for instance in [30, 36]), so that the algorithm also finds a local minimizer of the  $\text{UGW}_\varepsilon$  problem. In the Balanced-GW case, this can be explained by the fact that this scheme is equivalent to a mirror descent algorithm [36]. Minimizing the lower bound of (24) with respect to either  $\pi$  or  $\gamma$  is non-trivial for an arbitrary  $\varphi$ . We restrict our attention to the Kullback-Leibler case  $D_\varphi = \rho \text{KL}$  with  $\rho > 0$ , which can be addressed by solving a regularized and convex unbalanced problem as studied in [11, 35]. It is explained in the following proposition.

**Proposition 5.** *For a fixed  $\gamma$ , the optimal  $\pi$  minimizing*

$$\min_{\pi} \mathcal{F}(\pi, \gamma) + \varepsilon \text{KL}(\pi \otimes \gamma | (\mu \otimes \nu)^{\otimes 2})$$

*is the solution of*

$$\min_{\pi} \int c_\gamma^\varepsilon(x, y) d\pi(x, y) + \rho m(\gamma) \text{KL}(\pi_1 | \mu) + \rho m(\gamma) \text{KL}(\pi_2 | \nu) + \varepsilon m(\gamma) \text{KL}(\pi | \mu \otimes \nu),$$

*where  $m(\gamma) \stackrel{\text{def.}}{=} \gamma(X \times Y)$  is the total mass of  $\gamma$ , and where we define the cost and weight associated to  $\gamma$  as*

$$\begin{aligned} c_\gamma^\varepsilon(x, y) &\stackrel{\text{def.}}{=} \int \lambda(\Gamma(x, \cdot, y, \cdot)) d\gamma + \rho \int \log\left(\frac{d\gamma_1}{d\mu}\right) d\gamma_1 + \rho \int \log\left(\frac{d\gamma_2}{d\nu}\right) d\gamma_2 \\ &\quad + \varepsilon \int \log\left(\frac{d\gamma}{d\mu d\nu}\right) d\gamma. \end{aligned}$$

*Proof.* First note that  $\mathcal{F}(\gamma, \pi) = \mathcal{F}(\pi, \gamma)$  so that minimizing with the first or the second argument gives the same solution. The rest follows from the relation (proved in Appendix A)

$$\text{KL}(\pi_1 \otimes \gamma_1 | \mu \otimes \mu) = m(\gamma) \text{KL}(\pi_1 | \mu) + m(\pi) \text{KL}(\gamma_1 | \mu) + (m(\gamma) - m(\mu))(m(\pi) - m(\mu)),$$

and also from

$$\text{KL}(\pi_1|\mu) = \int \log\left(\frac{d\gamma_1}{d\mu}\right) d\gamma_1 - (m(\gamma) - m(\mu)).$$

Similar formulas hold for  $(\pi_2, \gamma_2)$  and  $(\pi, \gamma)$ .  $\square$

Computing the cost  $c_\gamma^\varepsilon$  for spaces  $X$  and  $Y$  of  $n$  points requires in general  $O(n^4)$  operations and a  $O(n^4)$  memory footprint. However, as explained for instance in [29], for the special case  $\lambda(t) = t^2$ , this cost is reduced to  $O(n^3)$  and the memory footprint to  $O(n^2)$ , which allows to scale the method to larger problems. This is the cost we consider in the numerical simulations.

The resulting alternate minimization method is detailed in Algorithm 1. It makes use of the unbalanced Sinkhorn algorithm of [11, 35] as sub-iterations and is initialized using  $\pi = \mu \otimes \nu / \sqrt{m(\mu)m(\nu)}$ . This Sinkhorn algorithm operates over a pair of continuous functions (so-called Kantorovitch potentials)  $f_s(x)$  and  $g_s(y)$ . For discrete spaces  $X$  and  $Y$  of size  $n$ , these functions are stored in vectors of size  $n$ , and that integral involved in the updates becomes a sum. Each iteration of Sinkhorn thus has a cost  $n^2$ , and all the involved operation can be efficiently mapped to parallelizable GPU routines as detailed in [11].

There is an extra scaling step after computing  $\pi_{t+1}$  involving the mass  $m(\pi_t)$ . It corresponds to the scaling  $s$  of  $\pi \otimes \gamma$  such that  $m(\pi) = m(\gamma)$ , and we observe that this scaling is key not only to impose this mass equality but also to stabilize the algorithm. Otherwise we observed that  $m(\pi_{2t}) < 1 < m(\pi_{2t+1})$  and underflows whenever  $m(\pi) \rightarrow 0$  and  $m(\gamma) \rightarrow \infty$ .

---

**Algorithm 1** – UGW( $\mathcal{X}, \mathcal{Y}, \rho, \varepsilon$ )

---

**Input:** mm-spaces  $(\mathcal{X}, \mathcal{Y})$ , relaxation  $\rho$ , regularization  $\varepsilon$

**Output:** approximation  $(\pi, \gamma)$  minimizing 24

- 1: Initialize  $\pi_{t=0} = \mu \otimes \nu / \sqrt{m(\mu)m(\nu)}$ ,  $g_{s=0} = 0$ .
  - 2: **while**  $\pi_t$  has not converged **do**
  - 3:   Define  $c \leftarrow c_{\pi_t}^\varepsilon$ ,  $\rho_t \leftarrow m(\pi_t)\rho$ ,  $\varepsilon_t \leftarrow m(\pi_t)\varepsilon$
  - 4:   **while**  $(f_s, g_s)$  has not converged **do**
  - 5:      $\forall x, f_{s+1}(x) \leftarrow -\frac{\varepsilon_t \rho_t}{\varepsilon_t + \rho_t} \log \left( \int e^{\frac{g_s(y) - c(x,y)}{\varepsilon_t}} d\nu(y) \right)$
  - 6:      $\forall y, g_{s+1}(y) \leftarrow -\frac{\varepsilon_t \rho_t}{\varepsilon_t + \rho_t} \log \left( \int e^{\frac{f_{s+1}(x) - c(x,y)}{\varepsilon_t}} d\mu(x) \right)$
  - 7:   Update  $\pi_{t+1}(x, y) \leftarrow \exp \left[ \frac{f_{s+1}(x) + g_{s+1}(y) - c(x,y)}{\varepsilon_t} \right] \mu(x) \nu(y)$
  - 8:   Rescale  $\pi_{t+1} \leftarrow \sqrt{m(\pi_t)/m(\pi_{t+1})} \pi_{t+1}$
  - 9: Return  $(\pi, \gamma) = (\pi_t, \pi_{t+1})$ .
- 

Note also that balanced GW is recovered as a special case when setting  $\rho \rightarrow +\infty$ , so that  $\rho_t/(\varepsilon_t + \rho_t) \rightarrow 1$  should be used in the iterations. In order to speed up Sinkhorn inner-loops, especially for small values of  $\varepsilon$ , one can use linear extrapolation [38] or non-linear Anderson acceleration [34].



## 5 Numerical experiments

This section presents numerical simulations on synthetic examples, to highlight the qualitative behavior of UGW with respect to mass variation and outliers. In all these experiments,  $\mu$  and  $\nu$  are probability distributions, which allows us to compare GW with UGW.

**Robustness to imbalanced classes.** In this first example, we take  $X = Y = \mathbb{R}^2$  and consider  $\mathcal{E}, \mathcal{C}$  and  $\mathcal{S}$  to be uniform distributions on an ellipse, a disk and a square. Figure 1 contrasts the transportation plan obtained by GW and UGW for a fixed  $\mu = 0.5\mathcal{E} + 0.5\mathcal{C}$  and  $\nu$  obtained using two different mixtures of  $\mathcal{E}$  and  $\mathcal{S}$ . The black segments show the largest entries of the transportation matrix  $\pi$ , for a sub-sampled set of points (to ease visibility), thus effectively displaying the matching induced by the plan. Furthermore, the width of the dots are scaled according to the mass of the marginals  $\pi_1 \approx \mu$  and  $\pi_2 \approx \nu$ , i.e. the smaller the point, the smaller is the amount of transported mass. This figure shows that the exact conservation of mass imposed by GW leads to a poor geometrical matching of the shapes which have different global mass. As this should be expected, UGW recovers coherent matchings. We suspect the alternate minimization algorithm was able to find the global minimum in these cases.

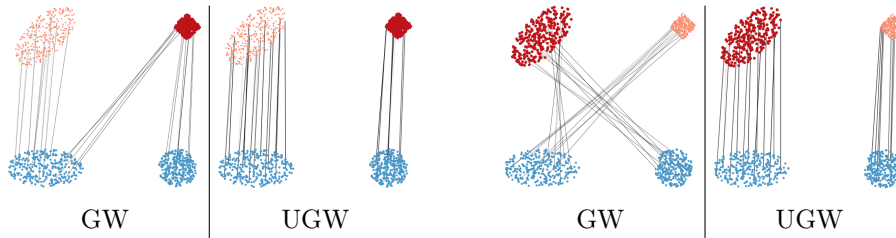


Figure 1: GW vs. UGW transportation plan, using  $\nu = 0.3\mathcal{E} + 0.7\mathcal{S}$  on the left, and  $\nu = 0.7\mathcal{E} + 0.3\mathcal{S}$  on the right.

**Influence of  $\varepsilon$  and debiasing.** This figure (and the following ones) does not show the influence of  $\varepsilon$  (which is set of a low value  $\varepsilon = 10^{-2}$  on a domain  $[0, 1]^2$ ). This influence is similar to those of classical OT, namely that it introduces an extra diffusion bias. This bias can be corrected by computing a debiased cost  $\text{UGW}_\varepsilon(\mu, \nu) - \text{UGW}_\varepsilon(\mu, \mu)/2 - \text{UGW}_\varepsilon(\nu, \nu)/2 + \frac{\varepsilon}{2}(m(\mu)^2 - m(\nu)^2)^2$ . While this debiasing is shown to lead to a valid divergence for W in [18] and UW in [35], we leave its study for UGW for future works.

**Robustness to outlier** Figure 2 shows another experiment on a 2-D dataset, using the same display convention as Figure 1. It corresponds to the two moons dataset with additional outliers (displayed in cyan). Decreasing the value of  $\rho$

(thus allowing for more mass creation/destruction in place of transportation) is able to reduce and even remove the influence of the outliers, as expected. Furthermore, using small values of  $\rho$  tends to favor “local structures”, which is a behavior quite different from UW (2). Indeed, for UW,  $\rho \rightarrow 0$  sets to zero all the mass of  $\pi$  outside of the diagonal (points are not transported), while for UGW, it is rather pairs of points with dissimilar pairwise distances which cannot be transported together.

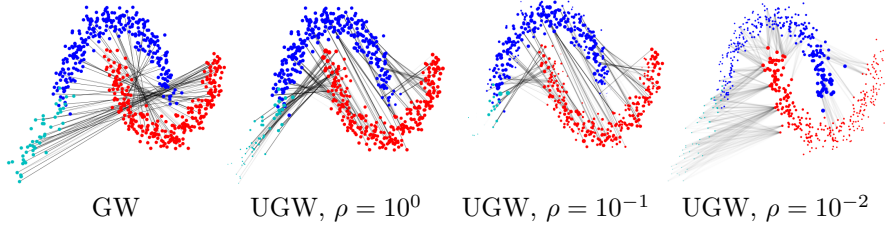


Figure 2: GW and UGW applied to two moons with outliers.

**Graph matching.** We now consider two graphs  $(X, Y)$  equipped with their respective geodesic distances. These graphs correspond to points embedded in  $\mathbb{R}^2$ , and the length of the edges corresponds to their Euclidean length. These two synthetic graphs are close to be isometric, but differ by addition or modification of small sub-structures. The colors  $c(x)$  are defined on the “source” graph  $X$  and are mapped by an optimal plan  $\pi$  on  $y \in Y$  to a color  $\frac{1}{\pi_1(y)} \int_X c(x) d\pi(x, y)$ . This allows to visualize the matching induced by GW and UGW for a varying  $\rho$ , as displayed in Figure 3.

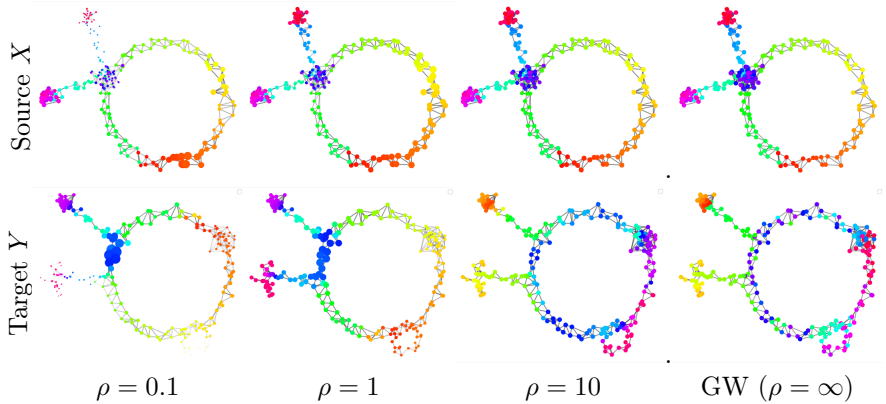


Figure 3: comparison of UGW and GW for graph matching.

For large values of  $\rho$ , UGW behaves similarly to GW, thus producing irregular matchings which do not preserve the overall geometry of the shapes. In sharp

contrast, for smaller values of  $\rho$  (e.g.  $\rho = 10^{-1}$ ), some fine scale structures (such as the target’s small circle) are discarded, and UGW is able to produce a meaningful partial matching of the graphs. For intermediate values ( $\rho = 10^0$ ), we observe that the two branches and the blue cluster of the source are correctly matched to the target, while for GW the blue points are scattered because of the marginal constraint.

## 6 Conclusion

This paper defines two Unbalanced Gromov-Wasserstein formulations. We prove that they are both positive and definite. We provide a scalable, GPU-friendly algorithm to compute one of them, and show that the other is a distance between mm-spaces up to isometry. These divergences and distances allow for the first time to blend in a seamless way the transportation geometry of GW with creation and destruction of mass.

This hybridization is the key to unlock both theoretical and practical issues. It raises new questions on the metric properties of those divergences and distances, as well as the geodesic structure that it might induce. It also offers new perspectives on the extension of GW methods to ML applications.

## Acknowledgements

The works of Thibault Séjourné and Gabriel Peyré is supported by the ERC grant NORIA.

## References

- [1] David Alvarez-Melis and Tommi S Jaakkola. Gromov-wasserstein alignment of word embedding spaces. *arXiv preprint arXiv:1809.00013*, 2018.
- [2] David Alvarez-Melis, Stefanie Jegelka, and Tommi S Jaakkola. Towards optimal transport with global invariances. In *The 22nd International Conference on Artificial Intelligence and Statistics*, pages 1870–1879. PMLR, 2019.
- [3] Martin Arjovsky, Soumith Chintala, and Léon Bottou. Wasserstein GAN. *arXiv preprint arXiv:1701.07875*, 2017.
- [4] Alexander M Bronstein, Michael M Bronstein, and Ron Kimmel. Generalized multidimensional scaling: a framework for isometry-invariant partial surface matching. *Proceedings of the National Academy of Sciences*, 103(5):1168–1172, 2006.
- [5] Charlotte Bunne, David Alvarez-Melis, Andreas Krause, and Stefanie Jegelka. Learning generative models across incomparable spaces. *arXiv preprint arXiv:1905.05461*, 2019.

- [6] Dmitri Burago, Iu D Burago, Yuri Burago, Sergei A Ivanov, and Sergei Ivanov. *A course in metric geometry*, volume 33. American Mathematical Soc., 2001.
- [7] Rainer E Burkard, Eranda Cela, Panos M Pardalos, and Leonidas S Pitsoulis. The quadratic assignment problem. In *Handbook of combinatorial optimization*, pages 1713–1809. Springer, 1998.
- [8] Laetitia Chapel, Mokhtar Z Alaya, and Gilles Gasso. Partial gromov-wasserstein with applications on positive-unlabeled learning. *arXiv preprint arXiv:2002.08276*, 2020.
- [9] Lenaïc Chizat and Francis Bach. On the global convergence of gradient descent for over-parameterized models using optimal transport. In *Advances in neural information processing systems*, pages 3036–3046, 2018.
- [10] Lenaïc Chizat, Gabriel Peyré, Bernhard Schmitzer, and François-Xavier Vialard. An interpolating distance between optimal transport and fisher-rao metrics. *Foundations of Computational Mathematics*, 18(1):1–44, 2018.
- [11] Lenaïc Chizat, Gabriel Peyré, Bernhard Schmitzer, and François-Xavier Vialard. Scaling algorithms for unbalanced transport problems. *to appear in Mathematics of Computation*, 2018.
- [12] Lénaïc Chizat, Gabriel Peyré, Bernhard Schmitzer, and François-Xavier Vialard. Unbalanced optimal transport: Dynamic and kantorovich formulations. *Journal of Functional Analysis*, 274(11):3090–3123, 2018.
- [13] Samir Chowdhury and Tom Needham. Gromov-wasserstein averaging in a riemannian framework. In *Proceedings of the IEEE/CVF Conference on Computer Vision and Pattern Recognition Workshops*, pages 842–843, 2020.
- [14] Luca Cosmo, Emanuele Rodolà, Michael M Bronstein, Andrea Torsello, Daniel Cremers, and Y Sahillioglu. Shrec’16: Partial matching of deformable shapes. *Proc. 3DOR*, 2(9):12, 2016.
- [15] Nicolas Courty, Rémi Flamary, and Devis Tuia. Domain adaptation with regularized optimal transport. In *Joint European Conference on Machine Learning and Knowledge Discovery in Databases*, pages 274–289. Springer, 2014.
- [16] Marco Cuturi. Sinkhorn distances: Lightspeed computation of optimal transport. In *Adv. in Neural Information Processing Systems*, pages 2292–2300, 2013.
- [17] Jean Feydy, Pierre Roussillon, Alain Trounev, and Pietro Gori. Fast and scalable optimal transport for brain tractograms. In *International Conference on Medical Image Computing and Computer-Assisted Intervention*, pages 636–644. Springer, 2019.

- [18] Jean Feydy, Thibault Séjourné, François-Xavier Vialard, Shun-ichi Amari, Alain Trounev, and Gabriel Peyré. Interpolating between optimal transport and mmd using sinkhorn divergences. In *The 22nd International Conference on Artificial Intelligence and Statistics*, pages 2681–2690, 2019.
- [19] Alessio Figalli. The optimal partial transport problem. *Archive for rational mechanics and analysis*, 195(2):533–560, 2010.
- [20] Charlie Frogner, Chiyuan Zhang, Hossein Mobahi, Mauricio Araya, and Tomaso A Poggio. Learning with a Wasserstein loss. In *Advances in Neural Information Processing Systems*, pages 2053–2061, 2015.
- [21] Justin Gilmer, Samuel S Schoenholz, Patrick F Riley, Oriol Vinyals, and George E Dahl. Neural message passing for quantum chemistry. In *Proceedings of the 34th International Conference on Machine Learning-Volume 70*, pages 1263–1272. JMLR. org, 2017.
- [22] Steven Gold and Anand Rangarajan. A graduated assignment algorithm for graph matching. *IEEE Transactions on pattern analysis and machine intelligence*, 18(4):377–388, 1996.
- [23] Steven Gold, Anand Rangarajan, et al. Softmax to softassign: Neural network algorithms for combinatorial optimization. *Journal of Artificial Neural Networks*, 2(4):381–399, 1996.
- [24] Edouard Grave, Armand Joulin, and Quentin Berthet. Unsupervised alignment of embeddings with wasserstein procrustes. In *The 22nd International Conference on Artificial Intelligence and Statistics*, pages 1880–1890, 2019.
- [25] John Lee, Nicholas P Bertrand, and Christopher J Rozell. Parallel unbalanced optimal transport regularization for large scale imaging problems. *arXiv preprint arXiv:1909.00149*, 2019.
- [26] Matthias Liero, Alexander Mielke, and Giuseppe Savaré. Optimal entropy-transport problems and a new hellinger–kantorovich distance between positive measures. *Inventiones mathematicae*, pages 1–149, 2015.
- [27] Matthias Liero, Alexander Mielke, and Giuseppe Savaré. Optimal transport in competition with reaction: The hellinger–kantorovich distance and geodesic curves. *SIAM Journal on Mathematical Analysis*, 48(4):2869–2911, 2016.
- [28] Facundo Mémoli. Gromov–wasserstein distances and the metric approach to object matching. *Foundations of computational mathematics*, 11(4):417–487, 2011.
- [29] Gabriel Peyré, Marco Cuturi, and Justin Solomon. Gromov-wasserstein averaging of kernel and distance matrices. In *International Conference on Machine Learning*, pages 2664–2672, 2016.

- [30] Anand Rangarajan, Alan Yuille, and Eric Mjolsness. Convergence properties of the softassign quadratic assignment algorithm. *Neural Computation*, 11(6):1455–1474, 1999.
- [31] Iwegen Redko, Titouan Vayer, Rémi Flamary, and Nicolas Courty. Co-optimal transport. *arXiv preprint arXiv:2002.03731*, 2020.
- [32] Emanuele Rodola, Alex M Bronstein, Andrea Albarelli, Filippo Bergamasco, and Andrea Torsello. A game-theoretic approach to deformable shape matching. In *2012 IEEE Conference on Computer Vision and Pattern Recognition*, pages 182–189. IEEE, 2012.
- [33] Grant Rotskoff, Samy Jelassi, Joan Bruna, and Eric Vanden-Eijnden. Global convergence of neuron birth-death dynamics. *arXiv preprint arXiv:1902.01843*, 2019.
- [34] Damien Scieur, Alexandre d’Aspremont, and Francis Bach. Regularized nonlinear acceleration. In *Advances In Neural Information Processing Systems*, pages 712–720, 2016.
- [35] Thibault Séjourné, Jean Feydy, François-Xavier Vialard, Alain Trounev, and Gabriel Peyré. Sinkhorn divergences for unbalanced optimal transport. *arXiv preprint arXiv:1910.12958*, 2019.
- [36] J. Solomon, G. Peyré, V. Kim, and S. Sra. Entropic metric alignment for correspondence problems. *ACM Transactions on Graphics (TOG)*, 35(4), 2016.
- [37] Karl-Theodor Sturm. The space of spaces: curvature bounds and gradient flows on the space of metric measure spaces. *arXiv preprint arXiv:1208.0434*, 2012.
- [38] Alexis Thibault, Lénaïc Chizat, Charles Dossal, and Nicolas Papadakis. Overrelaxed Sinkhorn-Knopp algorithm for regularized optimal transport. *arXiv preprint arXiv:1711.01851*, 2017.
- [39] Paul Tseng. Convergence of a block coordinate descent method for nondifferentiable minimization. *Journal of optimization theory and applications*, 109(3):475–494, 2001.
- [40] Titouan Vayer, Laetita Chapel, Rémi Flamary, Romain Tavenard, and Nicolas Courty. Fused gromov-wasserstein distance for structured objects: theoretical foundations and mathematical properties. *arXiv preprint arXiv:1811.02834*, 2018.
- [41] Cedric Villani. *Topics in C. Transportation*. Graduate studies in Math. AMS, 2003.
- [42] Hongteng Xu, Dixin Luo, and Lawrence Carin. Scalable gromov-wasserstein learning for graph partitioning and matching. In *Advances in neural information processing systems*, pages 3046–3056, 2019.

- [43] Hongteng Xu, Dixin Luo, Ricardo Henao, Svati Shah, and Lawrence Carin. Learning autoencoders with relational regularization. *arXiv preprint arXiv:2002.02913*, 2020.

## A Algorithmic details and formulas

### A.1 Properties of KL divergence

We present in this section an additional property on the quadratic-KL divergence which allows to reduce the computational burden to evaluate it by involving the computation of a standard KL divergence.

**Proposition 6.** *For any measures  $(\mu, \nu) \in \mathcal{M}_+(\mathcal{X})$ , one has*

$$\begin{aligned} \text{KL}(\mu \otimes \nu | \alpha \otimes \beta) &= m(\nu)\text{KL}(\mu | \alpha) + m(\mu)\text{KL}(\nu | \beta) \\ &\quad + (m(\mu) - m(\alpha))(m(\nu) - m(\beta)). \end{aligned} \quad (25)$$

*In particular,*

$$\text{KL}(\mu \otimes \mu | \nu \otimes \nu) = 2m(\mu)\text{KL}(\mu | \nu) + (m(\mu) - m(\nu))^2. \quad (26)$$

*Proof.* Assuming  $\text{KL}(\mu \otimes \nu | \alpha \otimes \beta)$  to be finite, one has  $\mu = f\alpha$  and  $\nu = g\beta$ . It reads

$$\begin{aligned} \text{KL}(\mu \otimes \nu | \alpha \otimes \beta) &= \int \log(f \otimes g) d\mu d\nu - m(\mu)m(\nu) + m(\alpha)m(\beta) \\ &= m(\nu) \int \log(f) d\mu + m(\mu) \int \log(g) d\nu \\ &\quad - m(\mu)m(\nu) + m(\alpha)m(\beta) \\ &= m(\nu) [\text{KL}(\mu | \alpha) + m(\mu) - m(\alpha)] \\ &\quad + m(\mu) [\text{KL}(\nu | \beta) + m(\nu) - m(\beta)] \\ &\quad - m(\mu)m(\nu) + m(\alpha)m(\beta) \\ &= m(\nu)\text{KL}(\mu | \alpha) + m(\mu)\text{KL}(\nu | \beta) \\ &\quad + m(\mu)m(\nu) - m(\nu)m(\alpha) - m(\mu)m(\beta) + m(\alpha)m(\beta) \\ &= m(\nu)\text{KL}(\mu | \alpha) + m(\mu)\text{KL}(\nu | \beta) \\ &\quad + (m(\mu) - m(\alpha))(m(\nu) - m(\beta)). \end{aligned}$$

□

### A.2 Discrete setting and formulas

To implement those algorithms, we represent mm-spaces in a discrete setting and write the index  $(p)$  with  $p \in \{1, 2\}$ . The set  $X^{(p)}$  becomes a set of  $N_{(p)}$  elements  $(x_i^{(p)})_i$  in some set  $E^{(p)}$  (e.g. nodes of a graph or points in  $\mathbb{R}^d$ ). The distance  $d_{(p)}$  is represented by the cost matrix  $C^{(p)}$  of dimension  $N_{(p)}^2$ . The measure  $\mu^{(p)}$  is encoded by a nonnegative  $N_{(p)}$ -dimensional vector. The cost and the measure respectively read

$$C_{ij}^{(p)} = C^{(p)}(x_i^{(p)}, x_j^{(p)}) \quad \text{and} \quad \mu^{(p)} = \sum_j \mu_j^{(p)} \delta_{x_j^{(p)}}.$$



In this setting any transport plan  $\pi = (\pi_{ij})$  is a  $N_{(1)}N_{(2)}$ -dimensional matrix where  $\pi_{ij}$  represents the mass transported from  $x_i^{(1)}$  to  $x_j^{(2)}$ . The discrete expression of the terms in  $\mathcal{L}$  now reads

$$\begin{aligned} \int \Gamma^2 d\pi d\pi &= \sum_{i,j,k,l} (C_{ij}^{(1)} - C_{kl}^{(2)})^2 \pi_{ik} \pi_{jl} \\ \rho D_\varphi(\pi_1 \otimes \pi_1 | \mu^{(1)} \otimes \mu^{(1)}) &= \rho \sum_{\substack{i,j \\ \mu_i^{(1)} \mu_j^{(1)} \neq 0}} \varphi\left(\frac{\pi_{1,i} \pi_{1,j}}{\mu_i^{(1)} \mu_j^{(1)}}\right) + \rho \varphi'_\infty \sum_{\substack{i,j \\ \mu_i^{(1)} \mu_j^{(1)} = 0}} \pi_{1,i} \pi_{1,j} \end{aligned}$$

where we define the marginals  $\pi_{1,k} \stackrel{\text{def.}}{=} \sum_j \pi_{kj}$  and  $\pi_{2,l} \stackrel{\text{def.}}{=} \sum_i \pi_{il}$ . For KL the second sum is always zero because  $\mu_i^{(p)} = 0$  imposes that  $\pi_{ij} = 0$ .

Concerning Sinkhorn, the stabilized computation involves a Log-Sum-Exp reduction that reads

$$f_i^{t+1} \leftarrow -\frac{\varepsilon \rho}{\varepsilon + \rho} LSE_j((g_j - T_{ij})/\varepsilon + \log(\mu_j^{(2)})) \quad (27)$$

where  $LSE_j$  is a reduction performed on the index  $j$ . It reads

$$LSE_j(C_{ij}) \stackrel{\text{def.}}{=} \log \left( \sum_j \exp(C_{ij} - \max_k C_{ik}) \right) + \max_k C_{ik}, \quad (28)$$

where the logarithm and exponential are pointwise operations.

## B UGW formulation and definiteness

We present in this section the proofs of the properties of our divergence UGW. We refer to Section 3 for the definition of the UGW formulation and its related concepts.

We first start with the existence of minimizers stated in Proposition 3. It illustrates in some sense that our divergence is well-defined.

**Proposition 7** (Existence of minimizers). *Assume  $(\mathcal{X}, \mathcal{Y})$  to be compact mm-spaces and that we either have*

1.  $\varphi$  superlinear, i.e  $\varphi'_\infty = \infty$
2.  $\lambda$  has compact sublevel sets in  $\mathbb{R}_+$  and  $2\varphi'_\infty + \inf \lambda > 0$

*Then there exists  $\pi \in \mathcal{M}_+(X \times Y)$  such that  $\text{UGW}(\mathcal{X}, \mathcal{Y}) = \mathcal{L}(\pi)$ .*

*Proof.* We adapt here from [26, Theorem 3.3]. The functional is lower semi-continuous as a sum of l.s.c terms. Thus it suffices to have relative compactness of the set of minimizers. Under either one of the assumptions, coercivity of the functional holds thanks to Jensen's inequality

$$\begin{aligned} \mathcal{L}(\pi) &\geq m(\pi)^2 \inf \lambda(\Gamma) + m(\mu)^2 \varphi\left(\frac{m(\pi)^2}{m(\mu)^2}\right) + m(\nu)^2 \varphi\left(\frac{m(\pi)^2}{m(\nu)^2}\right) \\ &\geq m(\pi)^2 \left[ \inf \lambda(\Gamma) + \frac{m(\mu)^2}{m(\pi)^2} \varphi\left(\frac{m(\pi)^2}{m(\mu)^2}\right) + \frac{m(\nu)^2}{m(\pi)^2} \varphi\left(\frac{m(\pi)^2}{m(\nu)^2}\right) \right]. \end{aligned}$$

As  $m(\pi) \rightarrow +\infty$  the right hand side converges to  $2\varphi'_\infty + \inf \lambda > 0$ , which under either one of the assumptions yields  $\mathcal{L}(\pi) \rightarrow +\infty$ , hence the coercivity. Thus we can assume there exists some  $M$  such that  $m(\pi) < M$ . Since the spaces are assumed to be compact, the Banach-Alaoglu theorem holds and gives relative compactness in  $\mathcal{M}_+(X \times Y)$ .

Take any sequence of plans  $\pi_n$  that approaches  $\text{UGW}(\mathcal{X}, \mathcal{Y}) = \inf \mathcal{L}(\pi)$ . Compactness gives that a subsequence  $\pi_{n_k}$  weak\* converges to some  $\pi^*$ . Because  $\mathcal{L}$  is l.s.c, we have  $\mathcal{L}(\pi^*) \leq \inf \mathcal{L}(\pi)$ , thus  $\mathcal{L}(\pi^*) = \inf \mathcal{L}(\pi)$ . The existence of such limit reaching the infimum gives the existence of a minimizer.  $\square$

Note that this formulation is nonnegative and symmetric because the functional  $\mathcal{L}$  is also nonnegative and symmetric in its inputs  $(\mathcal{X}, \mathcal{Y})$ . This formulation allows straightforwardly to prove the definiteness of UGW.

**Proposition 8** (Definiteness of UGW). *Assume that  $\varphi^{-1}(\{0\}) = \{1\}$  and  $\lambda^{-1}(\{0\}) = \{0\}$ . The following assertions are equivalent:*

1.  $\text{UGW}(\mathcal{X}, \mathcal{Y}) = 0$
2.  $\exists \pi \in \mathcal{M}_+(X \times Y)$  whose marginals are  $(\mu, \nu)$  such that  $d_X(x, x') = d_Y(y, y')$  for  $\pi \otimes \pi$ -a.e.  $(x, x', y, y') \in (X \times Y)^2$ .

3. There exists a mm-space  $(Z, d_Z, \eta)$  with full support and Borel maps  $\psi_X : Z \rightarrow X$  and  $\psi_Y : Z \rightarrow Y$ . such that  $(\psi_X)_\# \eta = \mu$ ,  $(\psi_Y)_\# \eta = \nu$  and  $d_Z = (\psi_X)^\# d_X = (\psi_Y)^\# d_Y$
4. There exists a Borel measurable bijection between the measures' supports  $\psi : \text{spt}(\mu) \rightarrow \text{spt}(\nu)$  with Borel measurable inverse such that  $\psi_\# \mu = \nu$  and  $d_Y = \psi^\# d_X$ .

*Proof.* Recall that (2)  $\Leftrightarrow$  (3)  $\Leftrightarrow$  (4) from [37, Lemma 1.10]. thus it remains to prove (1)  $\Leftrightarrow$  (2).

If there is such coupling plan  $\pi$  between  $(\mu, \nu)$  then one has  $\pi \otimes \pi$ -a.e. that  $\Gamma = 0$ , and all  $\varphi$ -divergences are zero as well, yielding a distance of zero a.e.

Assume now that  $\text{UGW}(\mathcal{X}, \mathcal{Y}) = 0$ , and write  $\pi$  an optimal plan. All terms of  $\mathcal{L}$  are positive, thus under our assumptions we have  $\Gamma = 0$ ,  $\pi_1 \otimes \pi_1 = \mu \otimes \mu$  and  $\pi_2 \otimes \pi_2 = \nu \otimes \nu$ . Thus we get that  $\pi$  has marginals  $(\mu, \nu)$  and that  $d_X(x, x') = d_Y(y, y')$   $\pi \otimes \pi$ -a.e.  $\square$

We end with the proof of Lemma 1.

**Lemma 4.** *One has*

$$\mathcal{L}(\pi) = \int_{X^2 \times Y^2} L_{\lambda(\Gamma)}(f \otimes f, g \otimes g) d\pi d\pi + \psi'_\infty(|(\mu \otimes \mu)^\perp| + |(\nu \otimes \nu)^\perp|).$$

*Proof.* Using Equation (21) with the Lebesgue decomposition and the definitions of reverse entropies and  $L_c$  from Section 2, one has

$$\begin{aligned} \mathcal{L}(\pi) &= \int_{X^2 \times Y^2} \lambda(\Gamma) d\pi d\pi + D_\varphi^\otimes(\pi_1 | \mu) + D_\varphi^\otimes(\pi_2 | \nu) \\ &= \int_{X^2 \times Y^2} \lambda(\Gamma) d\pi d\pi + D_\psi^\otimes(\mu | \pi_1) + D_\psi^\otimes(\nu | \pi_2) \\ &= \int_{X^2 \times Y^2} \lambda(\Gamma) d\pi d\pi + \int_{X^2} \psi(f \otimes f) d\pi_1 d\pi_1 + \int_{Y^2} \psi(g \otimes g) d\pi_2 d\pi_2 \\ &\quad + \psi'_\infty(|(\mu \otimes \mu)^\perp| + |(\nu \otimes \nu)^\perp|) \\ &= \int_{X^2 \times Y^2} L_{\lambda(\Gamma)}(f \otimes f, g \otimes g) d\pi d\pi + \psi'_\infty(|(\mu \otimes \mu)^\perp| + |(\nu \otimes \nu)^\perp|). \end{aligned}$$

$\square$

## C Conic formulation and metric properties

We present in this section the proofs of the properties mentioned in Section 3. We refer to Sections 2 and 3 for the definition of the conic formulation and its related concepts.

In this section we frequently use the notion of marginal for measures. For any sets  $E, F$ , we write  $\mathfrak{P}^{(E)} : E \times F \rightarrow E$  the **canonical projection** such that for any  $(x, y) \in E \times F$ ,  $\mathfrak{P}^{(E)}(x, y) = x$ . Consider two complete separable mm-spaces

$\mathcal{X} = (X, d_X, \mu)$  and  $\mathcal{Y} = (Y, d_Y, \nu)$ . Write  $\pi \in \mathcal{M}_+(X \times Y)$  a coupling plan, and define its marginals by  $\pi_1 = \mathfrak{P}_\#^{(X)}\pi$  and  $\pi_2 = \mathfrak{P}_\#^{(Y)}\pi$ . The definition of the marginals can also be seen by the use of test functions. In the case of  $\pi_1$  it reads for any test function  $\xi$

$$\int \xi(x) d\pi_1(x) = \int \xi(x) d\pi(x, y).$$

### C.1 Invariance to dilation and triangle inequality

We introduced the notion of dilation in section 3 which is key to prove the triangular inequality. We show this property and its consequences in this section.

**Lemma 5** (Invariance to dilation). *The problem CGW is invariant to dilations, i.e. for any  $\alpha \in \mathcal{U}_p(\mu, \nu)$ , we have  $\text{Dil}_v(\alpha) \in \mathcal{U}_p(\mu, \nu)$  and  $\mathcal{H}(\alpha) = \mathcal{H}(\text{Dil}_v(\alpha))$ .*

*Proof.* First we prove the stability of  $\mathcal{U}_p(\mu, \nu)$  under dilations. Take  $\alpha \in \mathcal{U}_p(\mu, \nu)$ . For any test function  $\xi$  defined on  $X$  we have

$$\int \xi(x) r^p d\text{Dil}_v(\alpha) = \int \xi(x) \left(\frac{r}{v}\right)^p \cdot v^p d\alpha = \int \xi(x) r^p d\alpha = \int \xi(x) d\mu(x).$$

Similarly we get  $\mathfrak{P}_\#^{(Y)}(s^q \text{Dil}_v(\alpha)) = \nu$ , thus  $\text{Dil}_v(\alpha) \in \mathcal{U}_p(\mu, \nu)$ .

It remains to prove the invariance of the functional. Recall that  $\mathcal{D}^q$  is  $p$ -homogeneous. It yields

$$\begin{aligned} \mathcal{H}(\text{Dil}_v(\alpha)) &= \int \mathcal{D}([d_X(x, x'), rr'], [d_Y(y, y'), ss'])^q d\text{Dil}_v(\alpha) d\text{Dil}_v(\alpha) \\ &= \int \mathcal{D}([d_X(x, x'), \frac{r}{v} \cdot \frac{r'}{v}], [d_Y(y, y'), \frac{s}{v} \cdot \frac{s'}{v}])^q v^p \cdot v^p d\alpha d\alpha \\ &= \int \frac{1}{v^{2p}} \mathcal{D}([d_X(x, x'), rr'], [d_Y(y, y'), ss'])^q v^{2p} d\alpha d\alpha \\ &= \int \mathcal{D}([d_X(x, x'), rr'], [d_Y(y, y'), ss'])^q d\alpha d\alpha \\ &= \mathcal{H}(\alpha) \end{aligned}$$

Both the functional and the constraint set are invariant, thus the whole CGW problem is invariant to dilations.  $\square$

The above lemma allows to normalize the plan such that one of its marginal is fixed to some value. Fixing a marginal allows to generalize the gluing lemma which is a key ingredient of the triangle inequality in optimal transport.

**Lemma 6** (Normalization lemma). *Assume there exists  $\alpha \in \mathcal{U}_p(\mu, \nu)$  such that  $\text{CGW}(\mathcal{X}, \mathcal{Y}) = \mathcal{H}(\alpha)$ . Then there exists  $\tilde{\alpha}$  such that  $\tilde{\alpha} \in \mathcal{U}_p(\mu, \nu)$  and  $\text{CGW}(\mathcal{X}, \mathcal{Y}) = \mathcal{H}(\tilde{\alpha})$  and whose marginal on  $\mathfrak{C}[Y]$  is  $\nu_{\mathfrak{C}[Y]} = \mathfrak{P}^{(\mathfrak{C}[Y])}_\# \tilde{\alpha} = \delta_{\circ_Y} + \mathfrak{p}_\#(\nu \otimes \delta_1)$ , where  $\mathfrak{p}$  is the canonical injection from  $Y \times \mathbb{R}_+$  to  $\mathfrak{C}[Y]$ .*

*Proof.* The proof is exactly the same as [26, Lemma 7.10] and is included for completeness. Take an optimal plan  $\alpha$ . Because the functional and the constraints are homogeneous in  $(r, s)$ , the plan  $\hat{\alpha} = \alpha + \delta_{\mathfrak{o}_X} \otimes \delta_{\mathfrak{o}_Y}$  verifies  $\hat{\alpha} \in \mathcal{U}_p(\mu, \nu)$  and  $\mathcal{H}(\hat{\alpha}) = \mathcal{H}(\alpha)$ . Indeed, because of this homogeneity the contribution  $\delta_{\mathfrak{o}_X} \otimes \delta_{\mathfrak{o}_Y}$  has  $(r, s) = (0, 0)$  which has thus no impact.

Considering  $\hat{\alpha}$  instead of  $\alpha$  allows to assume without loss of generality that the transport plan charges the apex, i.e. setting

$$S = \{[x, r], [y, s] \in \mathfrak{C}[X] \times \mathfrak{C}[Y], [y, s] = \mathfrak{o}_Y\}, \quad (29)$$

one has  $\omega_Y \stackrel{\text{def.}}{=} \alpha(S) \geq 1$ . Then we can define the following scaling

$$v([x, r], [y, s]) = \begin{cases} s & \text{if } s > 0 \\ \omega_Y^{-1/q} & \text{otherwise.} \end{cases} \quad (30)$$

We prove now that  $\text{Dil}_v(\hat{\alpha})$  has the desired marginal on  $\mathfrak{C}(Y)$  by considering test functions  $\xi([y, s])$ . We separate the integral into two parts with the set  $S$ , and write  $\hat{\alpha} = \hat{\alpha}|_S + \hat{\alpha}|_{S^c}$  their restrictions to  $S$  and  $S^c$  respectively. It reads

$$\begin{aligned} \int \xi([y, s]) d\text{Dil}_v(\hat{\alpha}) &= \int \xi([y, s/v]) v^p d\hat{\alpha} \\ &= \int \xi([y, s/v]) v^p d\hat{\alpha}|_S + \int \xi([y, s/v]) v^p d\hat{\alpha}|_{S^c} \\ &= \int \xi(\mathfrak{o}_Y) \omega_Y^{-1} d\hat{\alpha}|_S + \int \xi([y, s/s]) s^p d\hat{\alpha}|_{S^c} \\ &= \xi(\mathfrak{o}_Y) \cdot \omega_Y \cdot \omega_Y^{-1} + \int \xi([y, 1]) s^p d\hat{\alpha} \\ &= \xi(\mathfrak{o}_Y) + \int \xi(\mathfrak{p}(y, s)) d(\nu(y) \otimes \delta_1(s)) \\ &= \int \xi([y, s]) d(\delta_{\mathfrak{o}_Y} + \mathfrak{p}_\#(\nu \otimes \delta_1)), \end{aligned}$$

which is the formula of the desired marginal on  $\mathfrak{C}[Y]$ . Since  $\hat{\alpha} \in \mathcal{U}_p(\mu, \nu)$ , its dilation is also in  $\mathcal{U}_p(\mu, \nu)$ , and  $\mathcal{H}(\alpha) = \mathcal{H}(\hat{\alpha}) = \mathcal{H}(\text{Dil}_v(\hat{\alpha}))$ .  $\square$